Clim Dyn
DOI 10.1007/s00382-012-1436-7

# Towards a better understanding of changes in wintertime cold extremes over Europe: a pilot study with CNRM and IPSL atmospheric models

**Julien Cattiaux · Hervé Douville · Aurélien Ribes · Fabrice Chauvin · Chloé Plante**

Received: 28 October 2011 / Accepted: 23 June 2012


**Abstract** Recent winter seasons have evidenced that global warming does not exclude the occurrence of exceptionally cold and/or snowy episodes in the Northern mid-latitudes. The expected rarefaction of such events is likely to exacerbate both their societal and environmental impacts. This paper therefore aims to evaluate model uncertainties underlying the fate of wintertime cold extremes over Europe. Understanding why climate models (1) still show deficiencies in simulating present-day features and (2) differ in their responses under future scenarios for the twentyfirst century indeed constitutes a crucial challenge. Here we propose a weather-regime approach in order to separate the contributions of large-scale circulation and non-dynamical processes to biases or changes in the simulated mean and extreme temperatures. We illustrate our methodology from the wintertime occurrence of extremely cold days in idealized atmosphere-only experiments performed with two of the CMIP5 climate models (CNRM-CM5 and IPSL-CM5A-LR). First we find that most of the present-day temperature biases are due to systematic errors in non-dynamical processes, while the main features of the large-scale dynamics are well captured in such experiments driven by observed sea-surface temperatures, with the exception of a generalized underestimation of blocking episodes. Then we show that uncertainties associated with changes in large-scale circulation modulate the depletion in cold extremes under an idealized scenario for the late twentyfirst century. These preliminary results suggest that the original methodology proposed in this paper can be helpful for understanding spreads of larger model-ensembles when simulating the response of temperature extremes to climate change.

**Keywords** Global climate model · European temperatures · Temperature extremes · Intra-seasonal variability · Weather regimes

## 1 Introduction

Beyond the long-term global mean temperature increase, climate change may trigger disproportionate responses in regional temperature variability, especially extreme events (e.g., summer heat-waves, winter cold spells). Since such events generally cause the highest impacts on both societies and ecosystems, it is crucial to evaluate their evolution under a warmer climate as expected in the twentyfirst century, together with the associated uncertainties. At mid-latitudes, inter-annual to intra-seasonal fluctuations in the local weather are mostly driven by chaotic disturbances of the atmospheric dynamics, resulting from baroclinic instabilities underlying meridional temperature gradients. During wintertime season, the intensification of such gradients causes in particular a strongest day-to-day variability in surface temperatures. Hence, while the probability of regional-scale cold waves is expected to diminish under global warming (e.g., Kharin et al. 2007), they are likely to persist across mid-latitude land areas even until the end of the twentyfirst century (Kodra et al. 2011). In addition, as illustrated during recently observed cold spells in Europe

This paper is a contribution to the special issue on the IPSL and CNRM global climate and Earth System Models, both developed in France and contributing to the 5th coupled model intercomparison project.

J. Cattiaux (✉) · H. Douville · A. Ribes · F. Chauvin · C. Plante
Météo-France/CNRM-GAME,
42 avenue Gaspard Coriolis, 31057 Toulouse, France
e-mail: julien.cattiaux@meteo.fr

Published online: 15 July 2012

of winters 2009/10 (Cattiaux et al. 2010a, b; Ouzeau et al. 2011) and 2010/11, the increased societal vulnerability to such events may affect the public perception and continue to spur outbreaks of skepticism regarding the nature and causes of global warming. It is therefore important to better understand why models still show difficulties in simulating the basic dynamical and statistical features of present-day cold waves, and uncertainties in projecting their response to climate change scenarios.

Wintertime temperature variability over Europe is mostly controlled by the North-Atlantic Oscillation (NAO), generally defined as the main mode of variability in the daily large-scale circulation over this region (Hurrell et al. 2003, for a detailed review). The positive (negative) phase of the NAO is characterized by increased westerlies (easterlies) that carry warm (cold) air masses over the European continent (e.g., Thompson and Wallace 2001). Links between North-Atlantic atmospheric circulation and inter-annual to intra-seasonal variations in European temperatures, including cold extremes, have often been assessed trough weather-regime (e.g., Cassou et al. 2005) or weather-type (e.g., van den Besselaar et al. 2010) approaches. Such techniques consist in describing large-scale circulation fluctuations as transitions between a finite number of persisting and recurrent patterns. In particular wintertime cold outbreaks are generally associated with concurrent exceptional persistence of one regime, as during the cold winter 2009/10 characterized by a record occurrence of negative NAO conditions (Cattiaux et al. 2010a). The long-term increase in European temperatures has therefore legitimately been suspected to be induced by changes in frequencies of occurrence of weather regimes, especially after a remarkable spate of positive NAO winters in the 1980s–1990s (Corti et al. 1999; Palmer 1999; Gillett et al. 2003). However the return to less positive NAO winters after 1994/95 did not stop the long-term European warming, underlining the inability of large-scale circulation changes to explain the amplitude of both recent (Vautard and Yiou 2009) and future (Cattiaux et al. 2011) temperature trends.

Here we use a weather-regime approach in order to estimate which part of biases/changes in the representation of wintertime cold extremes by climate models can be attributed to large-scale circulation. Errors in the representation of large-scale dynamics by climate models can in particular result from their horizontal resolution (of the order of hundred km), insufficient for reproducing small-scales structures that are helpful in the maintenance of weather regimes (e.g., Cattiaux et al. 2012; Franzke et al. 2011). Thus we present an original methodology which linearly breaks up biases/changes into contributions of regime frequencies, within-regime distributions and other non-dynamical mechanisms that modulate European temperatures. Such non-dynamical mechanisms, which include physical processes linked to e.g., water vapor, clouds, snow or soil freezing, indeed constitute a potential source of systematic biases in climate models for the representation of temperature extremes given the complexity of associated feedbacks.

In this paper, we use idealized time-slice experiments run with two general circulation models (GCMs), CNRM-CM5 and IPSL-CM5A-LR, both designed for the Fifth Phase of the Coupled Model Inter-comparison Project (CMIP5). Models and reference datasets are presented in Sect. 2, as well as present-day evaluations and projected future changes in both mean and extreme wintertime temperatures. Section 3 describes the weather-regime approach and its relevance in the framework of this study, and details the breakdown methodology that separates dynamical from non-dynamical effects. An application to the projected depletion in extremely cold days over Europe is presented. Eventually, Sect. 4 summarizes main results and discusses potential prospects of this study.

## 2 Data

### 2.1 CNRM-CM5 and IPSL-CM5A-LR models

A complete and detailed description of CNRM-CM5 and IPSL-CM5A-LR (hereafter CNRM and IPSL) coupled ocean-atmosphere GCMs can be found in reference papers in this issue (Voldoire et al. 2012; Dufresne et al. 2012) and is not repeated here. In this study we use time-sliced atmosphere-only experiments, i.e. with prescribed sea-surface temperatures (SST) for both present-day and future climates as designed for the Atmospheric Model Inter-comparison Project (AMIP). Despite their possible limitations (e.g., Douville 2005), such AMIP-type experiments allow us to isolate the errors (present-day climate vs. observations) and uncertainties on changes (future vs. present-day climate) associated to the atmospheric component of coupled GCMs. In addition, the methodology presented in this paper aims to be applied to a larger number of both atmosphere-only and coupled ocean-atmosphere simulations.

The atmospheric component of CNRM-CM5 is the spectral ARPEGE-Climat GCM operating on a T127 linear grid (256 $\times$ 128 grid points) with 31 vertical levels and coupled to the ISBA land surface scheme (see Voldoire et al. (2012) in this issue for more details). The atmospheric component of IPSL-CM5A-LR is the LMDZ model operating on a regular 96 $\times$ 96 longitude-latitude grid with 39 vertical levels and coupled to the ORCHIDEE land surface scheme [details can also be found in this issue in Dufresne et al. (2012)]. Besides their dynamical core,

resolution and land-surface scheme, these models also have a different set of physical parameterizations and only share relatively close radiative schemes.

For both models we use daily outputs of wintertime (December–March, DJFM) daily minimum temperature (Tmin). In order to characterize the large-scale atmospheric circulation, we use the daily mean geopotential height at 500 hPa (Z500). The evaluation of present-day biases is based on the control AMIP experiment, whose prescribed monthly mean SSTs and radiative forcings are derived from 1979 to 2008 observations. The sensitivity to climate change is assessed using the AMIP-Future experiment as defined by the CMIP5 protocol (Taylor et al. 2007): the radiative forcing is unchanged and the SST forcing is the sum of 1979–2008 observations and climatological monthly anomalies, whose spatial pattern is derived from the CMIP3 model-ensemble projections and global average equals 4 K. While highly idealized, such an experiment constitutes a reasonable surrogate of future climate over Europe, since the indirect (i.e. ocean warming) effect dominates the direct (i.e. radiative) effect of increased greenhouse-gases concentrations on surface air temperature in this region (Déqué et al. 1998).

### 2.2 Observations and reanalyses

Biases in minimum temperatures are evaluated with respect to the Tmin in-situ observations provided by the European Climate Assessment and Dataset and interpolated onto a regular $0.5 \times 0.5^\circ$ grid [hereafter EOBS, Haylock et al. (2008)]. The reference for Z500 is taken from the NCEP/DOE reanalysis [hereafter NCEP2, Kanamitsu et al. (2002)] that also spans the AMIP period (1979–2008). In order to ease the comparison between both models and observations, all datasets are interpolated onto a common grid (without elevation corrections) with a first-order re-mapping scheme. We arbitrarily choose the T127 grid used in the CNRM atmospheric model, which is intermediate between all datasets and should be a medium resolution among all CMIP5 models.

### 2.3 Mean biases and future changes in temperatures

Mean biases in wintertime Tmin are presented for both models in Fig. 1. CNRM exhibits a generalized cold bias over Europe, with an average of $-0.5$ K over the whole domain (12°W–50°E; 36–71°N), and exceeding $-3$ K over mountainous regions (Alps, Scandinavian Alps and the Taurus located in Turkey). IPSL minimum temperatures are on average 1.1 K warmer than observations, with a warm bias south of 50°N and over Scandinavia, and a cold bias over North-Eastern Europe. Model behaviors over areas of complex orography are likely to be linked to their horizontal resolutions and to the lack of correction for the different elevations. Overall, biases are consistent with Voldoire et al. (2012) for CNRM and Menut et al. (2012) for IPSL.

Despite different present-day mean states, both models exhibit similar features in their sensitivity to "global warming", as defined as the difference between AMIP-Future and AMIP experiments (Fig. 2). On average, CNRM response is slightly warmer than IPSL (5.4 vs. 4.9 K), but spatial patterns are highly correlated ($r = 0.85$), in particular with a strong South-West–North-East gradient. The largest differences occur over mountainous regions, Scandinavia ($\sim$2 K) and Taurus ($\sim$4 K), which could be partly due to different snow feedbacks, especially at lower latitudes where solar radiation substantially impacts surface energy budgets in winter. The latter should nevertheless require further investigation.

### 2.4 Focus on cold spells

In addition to mean biases, we evaluate the ability of both models to reproduce observed cold extremes in AMIP experiments. For each grid point, extremely cold days are defined as days with a Tmin below the 10th percentile of the EOBS 1978–2007 distribution. The frequency of occurrence of such cold days over the whole period thus corresponds to the empirical Probability of exceeding the observed 10th Percentile (hereafter PP10). By design, a perfect representation of observed cold extremes would imply PP10 = 10 % at all grid points. For both models, EOBS-relative PP10 in AMIP experiments follow the mean bias at the first order: above (below) 10 % in areas of cold (warm) biases. On average over the whole European domain, CNRM (IPSL) produces 13.7 % (9.1 %) of extremely cold days.

Then we investigate the difference in cold extremes between AMIP and AMIP-Future experiments. For both models, PP10 are computed in the AMIP-Future experiment relative to the 10th percentile of the corresponding AMIP experiment. Not surprisingly, since this definition considers a fixed threshold (AMIP percentile), we find a large decrease in PP10 under future warming (Fig. 3). On average over the domain, only 0.5 % (1.5 %) of days are found to be extremely cold in AMIP-Future for the CNRM (IPSL) model. In other terms extremely cold days remain about three times more frequent in IPSL than CNRM, which is consistent with the larger temperature increase exhibited by the CNRM model. Interestingly, the spatial correlation between both responses is lower than for mean changes ($r = 0.46$), suggesting that temperature extremes do not necessarily scale on the mean of the distribution.

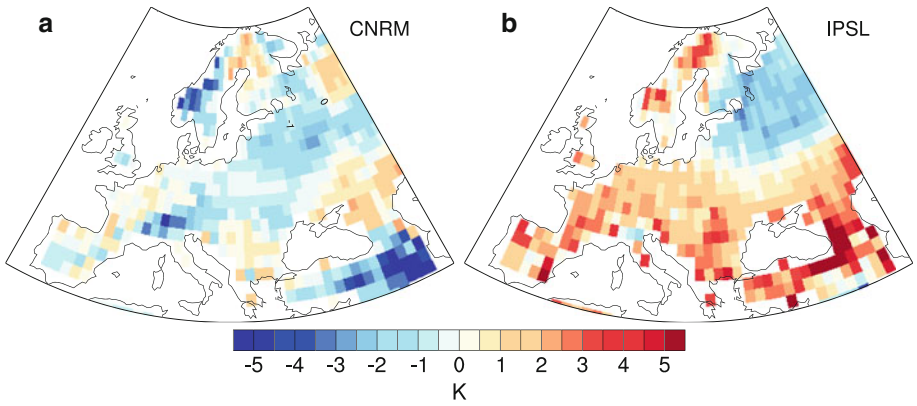


**Fig. 1** Mean departures from EOBS in wintertime Tmin for **a** CNRM and **b** IPSL. Units: K

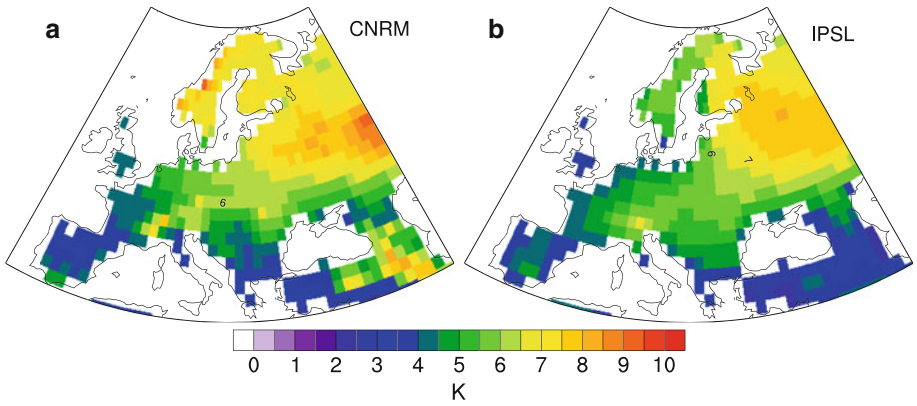


**Fig. 2** Mean differences between AMIP-Future and AMIP in wintertime Tmin for **a** CNRM and **b** IPSL. Units: K

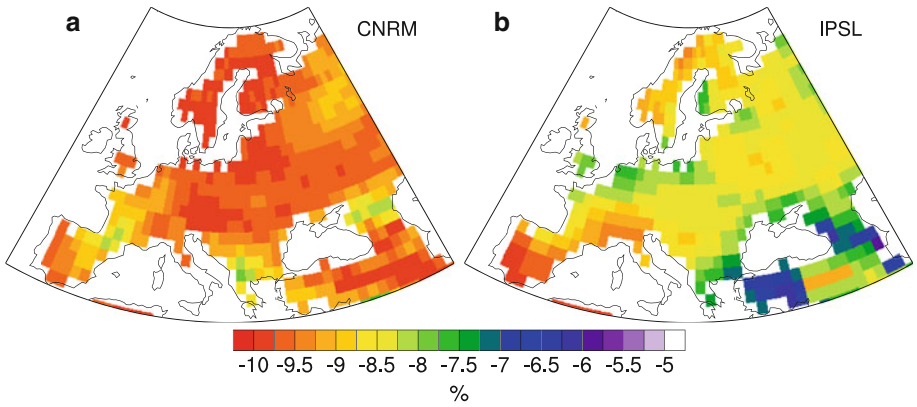


**Fig. 3** Same as Fig. 2 for PP10, represented as raw departures from 10 %. Units: %

### 2.5 Large-scale circulation

In association with the low-troposphere temperature increase, the Z500 tends to increase between AMIP and AMIP-Future, as a result of the low-troposphere thermal expansion. This is illustrated for both models in Fig. 4. On average over the whole North-Atlantic domain (90°W–30°E; 20–80°N), this elevation is larger for CNRM (127 m) than IPSL (100 m). In addition, despite a concurrent maximum over the Mediterranean area, the anomaly patterns differ: the largest changes in CNRM occur preferentially at low latitudes and over continents, while IPSL exhibits a strong North-Atlantic/Europe contrast and a limited elevation over the West-Atlantic. The following sections investigate to what extent such differences in Z500 fields are liable to modulate the European temperature response, both in terms of mean climate and extreme events.

## 3 Dynamical versus non-dynamical contributions

### 3.1 Weather-regime approach

In order to estimate the contribution of the large-scale atmospheric circulation to biases or changes in wintertime

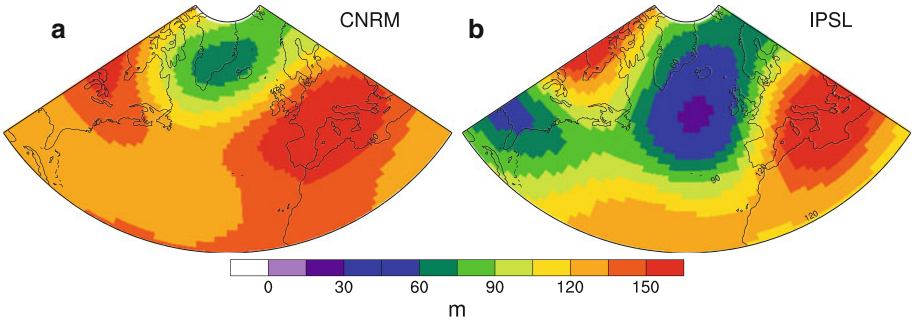


**Fig. 4** Same as Fig. 2 for Z500. Units: m

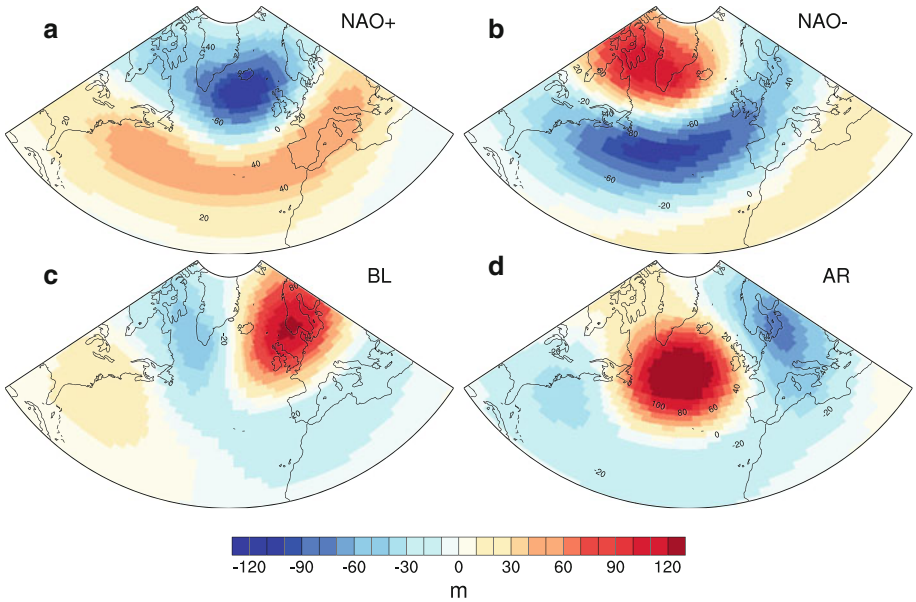


**Fig. 5** Wintertime weather regimes obtained from NCEP2 Z500: **a** NAO+, **b** NAO−, **c** Blocking and **d** Atlantic Ridge. Units: m

Tmin, we use a weather-regime approach. Such an approach has often been used in recent years (e.g., Vautard 1990), and consists in considering that the intra-seasonal variability of the North-Atlantic atmospheric circulation can be described as transitions between a limited number of recurrent and quasi-stationary states (or weather regimes). Here we calculate the weather regimes by computing the "k-means" clustering algorithm (Michelangeli et al. 1995) on the distribution of Z500 daily anomalies taken from NCEP2 reanalysis, over the domain used in Fig. 4 (90°W–30°E; 20–80°N). NCEP2 anomalies are calculated relative to the corresponding 1979–2008 climatology and only wintertime months (DJFM) are retained in the procedure. More details about this methodology can be found in this issue in Cattiaux et al. (2012). Eventually, we obtain the four well-known centroids described e.g., in Cassou (2008): the two phases of the North Atlantic Oscillation (NAO+, NAO−), the Scandinavian Blocking (BL) and the Atlantic Ridge (AR, Fig. 5).

For NCEP2, each day of DJFM 1979–2008 is attributed to the regime whose centroid is the closest to the day's Z500 anomaly in terms of Euclidean distance. Then, in order to retain robust and stationary episodes only and to avoid a too strong artificial constrain (sum equals one) between the relative frequencies of occurrence of the regimes, we arbitrarily apply a 0.25-minimal-correlation criterion (between centroid and day's Z500 anomaly) and a 3-day-persistence filter to the classification. This leads to discard about 20–25 % of all winter days, but we tested that our results would have been qualitatively similar if retaining all days. In the following we consider these "discarded" days as equivalent to a fifth regime: the so-called "bin" class.

In order to compare observed and simulated regimes, we use NCEP2 centroids as a common reference. Reasons for such a choice are discussed in this issue by Cattiaux et al. (2012) for the IPSL model, and basically rely on the fact that model centroids are generally close to observed ones (not shown). For both CNRM and IPSL models and both AMIP and AMIP-Future experiments, we compute wintertime Z500 anomalies relative to the AMIP climatology. Then, we attribute each day to the closest NCEP2 centroid

(Euclidean distance minimization), with both correlation and persistence criteria. In order to account for the thermal expansion of the troposphere in AMIP-Future (Fig. 4), the domain-averaged elevation of the Z500 field is removed before classifying days. Such a procedure, also applied in Cattiaux et al. (2010b) or Driouech et al. (2010), nevertheless retains the patterned response of Z500 to climate change, which is likely to project onto the regime frequencies. The differences in patterns of Fig. 4 are thus purposely accounted for by this methodology.

Frequencies of occurrence of weather regimes are presented in Fig. 6a. In the NCEP2 reanalysis, the period 1979–2008 is characterized by a high frequency ($\sim$25%) of NAO+ episodes (especially in the 1980s/1990s), while the three other regimes are rather equiprobable ($\sim$15–20 %). In AMIP experiments, both models represent the frequencies of both NAO+ and AR regimes quite well, while they underestimate BL and CNRM slightly overestimates NAO−. The BL underestimate is a common feature of many climate models which generally simulate a too strong and stable jet stream (e.g., Scaife et al. 2010). The 5 % confidence intervals—obtained by a bootstrap procedure over the 30 years of mean seasonal occurrences—indicate that the bin class is not overestimated by the models, which justifies the use of NCEP2 centroids as a common reference for classifications.

Figure 6b shows the difference between AMIP-Future and AMIP in mean regime occurrences. Both CNRM and IPSL models exhibit a significant increase in NAO+ frequency. Such large-scale dynamical response is consistent with previous findings in both CMIP2 (e.g., Stephenson et al. 2006) and CMIP3 (e.g., Cattiaux et al. 2011) projections, even if its robustness may be questioned by the wide spread in larger multi-model projections (Deser et al. 2010). In our study, the redistribution of the NAO+ increase among the other regimes significantly differs between CNRM and IPSL. CNRM (IPSL) produces a decrease (increase) in NAO−, while the IPSL decrease in AR frequency is significantly greater than for CNRM. BL responses are also contrasted, with an increase (decrease) for CNRM (IPSL).

Differences in frequencies between AMIP and AMIP-Future are directly linked to the mean Z500 difference shown in Fig. 4. The NAO+ increase is associated with the generally higher (lower) elevation over low (high) latitudes. Differences in evolutions of NAO− and AR frequencies result from the patterned responses: the CNRM (IPSL) pattern indeed appears slightly anti-correlated to the NAO− (AR) centroid of Fig. 5.

### 3.2 Weather regimes and temperatures

The relationship between weather regime occurrences and European temperatures has been addressed in many studies (e.g., Plaut and Simonnet 2001). In particular, intra-seaonal to seasonal temperature extremes are generally associated with an unusual persistence of one particular weather regime. The latter has been recently illustrated during the winter 2009/10 whose cold spells were caused by a record persistence of the NAO− regime (e.g., Cattiaux et al. 2010a). Here, in order to assess the link between weather regimes and European Tmin, we consider the following linear decomposition by writing the mean of a variable $X$ ($\overline{X}$) as the mean of regime-conditional means $x_k$ weighted by the frequencies of occurrence $f_k$:

$$\overline{X} = \frac{1}{N}\sum_{i\in\Omega} X_i = \sum_k f_k x_k, \tag{1}$$

with $\Omega$ the total ensemble of the $N$ days, $f_k = N_k/N$ the frequency of occurrence of the $k$th regime and $x_k$ the conditional mean to regime $k$ defined by:

$$x_k = \frac{1}{N_k}\sum_{i_k\in\Omega_k} X_{i_k}, \tag{2}$$

with $\Omega_k$ the ensemble of the $N_k$ days classified in the $k$th regime.

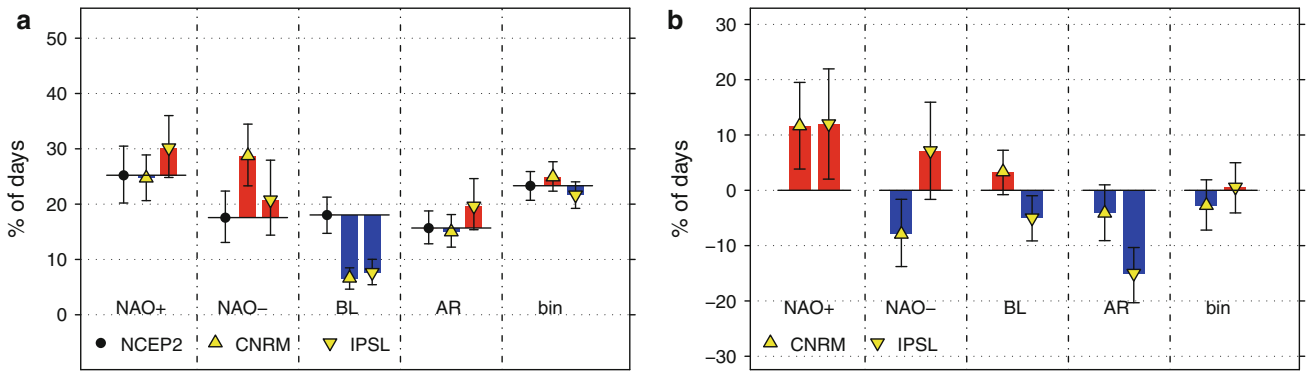


**Fig. 6** Mean frequencies of occurrence of weather regimes. **a** AMIP values for CNRM (*triangle*) and IPSL (*inverted triangle*) represented as departures from EOBS values (*filled circle*). **b** AMIP-Future values for CNRM and IPSL represented as departures from AMIP values. 95 %-confidence intervals obtained by bootstrap procedures are indicated. Units: %

In our case, the variable $X$ can represent either Tmin anomalies or PP10 in Eq. 1. In the former case, $\overline{X}$ corresponds to the average of Tmin anomaly over the whole period, and each $x_k$ represents the composite of Tmin anomalies within regime $k$. In the latter case, $\overline{X}$ corresponds to the mean probability to exceed the 10th Tmin percentile, $x_k$ the same probability of exceedance when placed in regime $k$, and Eq. 1 resembles a classical Bayes formula of conditional probabilities:

$$\overline{\mathrm{PP10}} \equiv P(T<T_{10}) = \sum_k P(\Omega_k)\cdot P(T<T_{10}|\Omega_k), \qquad (3)$$

with $P(\Omega_k) \equiv f_k$ the probability of regime $k$, and $P(T<T_{10}|\Omega_k) \equiv \mathrm{PP10}_k$ the conditional probability of exceedance to regime $k$. While the decomposition of Eq. 1 has already been applied to mean climate variables, such as surface winds (Boé et al. 2006; Najac et al. 2009), precipitation (Driouech et al. 2010) or temperature (Goubanova et al. 2010), its extension to probabilities of quantile exceedance has more rarely been performed (Cassou et al. 2005; Sanchez-Gomez et al. 2008). In this paper, the focus is therefore on the PP10 application.

Figure 7a–d shows the conditional PP10 for each regime in EOBS Tmin. The NAO+ regime, characterized by increased westerlies, brings mild air masses over Europe, which leads to a reduced frequency of extremely cold days over the whole domain ($\sim$3 % on average instead of 10 %), except over the Taurus area. Conversely, the NAO− regime brings polar air over Northern Europe, enhancing the probability of exceeding the 10th Tmin percentile north of 50°N. Both BL and AR are also associated with cold anomalies on average over Europe, and extremely cold days tend to be distributed among BL for Central Europe and AR for South-Western Europe. We verified that the conditional PP10 for the bin class is close to the mean probability of 10 %, which confirms the robustness of the regime partition in order to discriminate temperatures (not shown). Beyond their mean biases, both CNRM and IPSL models capture the observed partition of conditional PP10 among the four regimes (Fig. 7e–l). However, while IPSL overestimates the role of AR over France, patterns amplitudes are generally underestimated by both models, especially over Northern Europe in NAO− regime and over Central Europe in BL. The latter could indicate that weather regimes are less efficient at discriminating temperatures in models than in observations. This fact can either result from our choice to use NCEP2 centroids as references or suggest a weaker (at least different) relationship between circulations and temperatures in models. Such an issue is beyond the scope of our study.

### 3.3 Evaluating dynamical contributions

This section describes how contributions of large-scale dynamics to a difference of $\overline{X}$ can be estimated from Eq. 1. Indeed, if we consider for instance the difference in $\overline{X}$ between two time slices, e.g., future (index F) and present (P) climates, Eq. 1 indicates that:

$$\begin{aligned}\Delta^{F-P}\overline{X} = \overline{X}^F - \overline{X}^P &= \sum_k f_k^F x_k^F - \sum_k f_k^P x_k^P \\ &= \sum_k \left(f_k^F - f_k^P\right)x_k^P + \sum_k f_k^P\left(x_k^F - x_k^P\right) \\ &\quad + \sum_k \left(f_k^F - f_k^P\right)\left(x_k^F - x_k^P\right) \\ &= \underbrace{\sum_k \Delta f_k \cdot x_k^P}_{BC} + \underbrace{\sum_k f_k^P \cdot \Delta x_k}_{WC} + \underbrace{\sum_k \Delta f_k \cdot \Delta x_k}_{RES}, \qquad (4)\end{aligned}$$

where *BC* (between-class) represents the part of the total difference which is due to differences in frequencies of occurrence of weather regimes, and *WC* (within-class) the contribution of differences within the regimes, while *RES* ("Residual") is a mixing term. We arbitrarily formulate both *BC* and *WC* terms as functions of present-day values (respectively $x_k^P$ and $f_k^P$) in order to ease their interpretations. While Eq. 4 (or equivalent) has often been used for decomposing responses to climate change (e.g., Goubanova et al. 2010), is is worth noting that "future–present" can easily be replaced with "model–observations" in the difference of $\overline{X}$. Thus, in the following we carry on the methodology description using the climate change example, albeit keeping in mind than it could be applied to present-day biases as well.

The *WC* term in Eq. 4 is the most difficult to interpret, in particular because $\Delta x_k$ terms can contain both dynamical and non-dynamical sources. Indeed, the subset of the Z500 distribution corresponding to days placed in regime $k$ (hereafter $d_k$) may differ between present and future, e.g., due to a slight shift of the mean centroid $k$. In addition, the relationship between $X$ and the Z500 may be modified in the future, leading to different $x_k$ for equal $d_k$. In order to distinguish these two contributions in the term *WC*, we introduce a transfer function $\Phi$ such as:

$$\forall k \quad x_k = \Phi(d_k), \qquad (5)$$

i.e which associates a mean value of $X$ to a distribution $d$ of Z500 anomalies. $\Phi$ can be interpreted as the non-dynamical mechanisms that convert the influence of the large-scale circulation on the European temperatures, including surface conditions (e.g., sea-surface temperatures, soil moisture, snow) and radiative feedbacks (e.g., clouds, aerosols). It is worth noting that, in reality, large-scale circulation and such

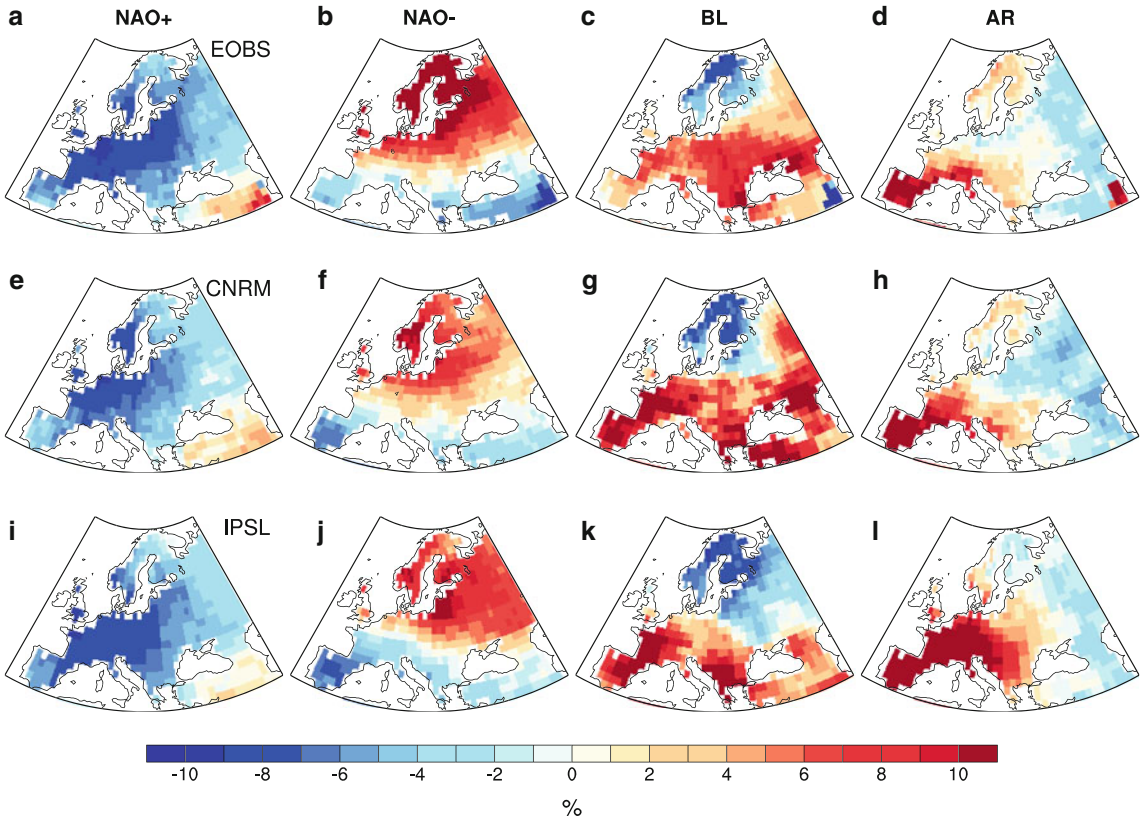


**Fig. 7** Weather-regimes conditional PP10 for **a–d** EOBS, **e–h** CNRM (AMIP) and **i–l** IPSL (AMIP). PP10 values are represented as raw departures from 10 %. For CNRM and IPSL, mean biases are removed (see details in text). Units: %

regional processes are not independent, so that the artificial split of Eq. 5 should nevertheless be carefully interpreted. Equation 1 can be rewritten as follows:

$$\overline{X} = \sum_k f_k \Phi(d_k), \tag{6}$$

and since:

$$\begin{aligned}\Delta x_k &= \Phi^F\left(d_k^F\right) - \Phi^P\left(d_k^P\right) \\ &= \left[\Phi^F\left(d_k^F\right) - \Phi^P\left(d_k^F\right)\right] + \left[\Phi^P\left(d_k^F\right) - \Phi^P\left(d_k^P\right)\right],\end{aligned} \tag{7}$$

the *WC* term can be split in two parts and Eq. 4 becomes:

$$\begin{aligned}\Delta\overline{X} = &\underbrace{\sum_k \Delta f_k \cdot \Phi^P\left(d_k^P\right)}_{BC} + \underbrace{\sum_k f_k^P \cdot \left[\Phi^P\left(d_k^F\right) - \Phi^P\left(d_k^P\right)\right]}_{WCd} \\ &+ \underbrace{\sum_k f_k^P \cdot \left[\Phi^F\left(d_k^F\right) - \Phi^P\left(d_k^F\right)\right]}_{WC\Phi} + \underbrace{\sum_k \Delta f_k \cdot \Delta[\Phi(d_k)]}_{RES},\end{aligned} \tag{8}$$

where *WCd* represents the part due to differences in $d_k$ only, and *WC*Φ represents the part due to differences in the transfer function Φ only. Concretely the term $\Phi^P(d_k^F)$ represents the mean value of $X$ that would produce the present non-dynamical mechanisms from daily circulations of the future. It is the most difficult term to estimate in order to derive the full composite. A practical way to do it is to consider:

$$\Phi^P\left(d_k^F\right) \equiv \Phi^P\left(\widetilde{d_k^P}\right), \tag{9}$$

where $\widetilde{d_k^P}$ represents the subset of the present-day Z500 distribution which is the closest to the future $d_k^F$. In other terms $\widetilde{d_k^P}$ are the flow-analogs of $d_k^F$ in the present-day circulations, as defined by Lorenz (1969) and used in a bunch of recent studies (e.g., Vautard and Yiou 2009). We arbitrarily introduce the mixed term $\Phi^P(d_k^F)$ in Eq. 7 (instead of, e.g., $\Phi^F(d_k^P)$), because it allows, as in Eq. 4, to consider present-day as the reference: the *WCd* term is formulated as a function of $\Phi^P$, and the *WC*Φ term uses $d_k^F = \widetilde{d_k^P}$, thus seeking analogs of future states in the "reference" set of present-day states.

Thus, for both CNRM and IPSL models and for each day in AMIP-Future experiment, we select days with the most analog Z500 field in the AMIP experiment. Analog days are sought in all AMIP years, but in the same "month" (31-day moving window). The analogy is assessed by maximizing the spatial correlation, but other metrics would not have substantially changed the selection [tested

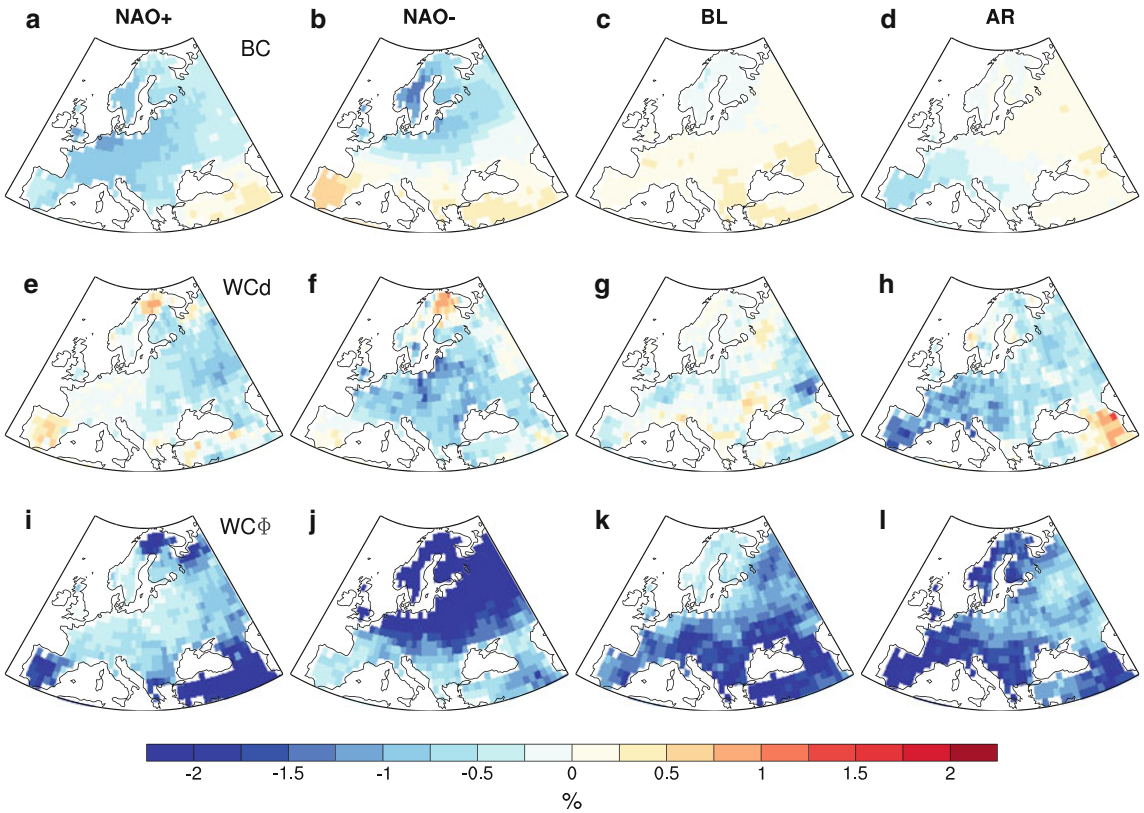


**Fig. 8** Decomposition of the CNRM AMIP-Future–AMIP difference in PP10 according to Eq. 8. **a–d** *BC* terms for each regime, respectively NAO+, NAO−, BL and AR. **e–h** Same for *WCd* terms. **i–l** Same for *WCΦ* terms. PP10 values are represented as raw departures from 10 %. The remaining terms of Eq. 8 corresponding to the bin class and/or to the residual *RES* are not shown. Units: %

in Cattiaux et al. (2011)]. In order to have subsets $d_k^F$ and $\widetilde{d_k^P}$ of same size, we only retain one analog per day (the first one). Even though there is no methodological reason to constrain the seek of $d_k^F$ analogs to days belonging to $d_k^P$ (i.e. placed in the same regime), we find that $\sim$85 % of $\widetilde{d_k^P}$ actually lie in $d_k^P$. This confirms (1) the robustness of the weather-regime approach to discriminate daily circulations and (2) the quality of the selected flow-analogues, which are both strong requirements of our methodology.

### 3.4 Application to future changes in PP10

The breakdown of Eq. 8 can be applied to both Tmin anomalies or PP10 variables ($\overline{X}$), and to both present-day biases or future changes ($\Delta$). As previously discussed, the focus on PP10 seems promising, especially because extreme cold days are remarkably geographically partitioned among the four regimes (Fig. 7a–d). In addition, applying Eq. 8 to present-day biases indicates that for both models the contribution of both *BC* and *WCd* terms are minor (not shown), which means in particular that biases in regimes' frequencies exhibited in Fig. 6a are dominated by non-dynamical biases for the representation of temperature extremes. Such a conclusion should however be moderated given the use of AMIP-type experiments, in which prescribed SST inhibit the influence of systematic atmospheric biases on seasonal mean large-scale circulation. At this timescale, Eq. 8 should be more fruitful when applied to coupled ocean-atmosphere models. In this section, we therefore decided to focus on breaking up future changes in PP10.

Figures 8 and 9 show *BC*, *WCd* and *WCΦ* individual terms for each regime, respectively for CNRM and IPSL models. Residual terms (*RES*) and/or contributions of the bin class are omitted for convenience, but we verified that no major signal appears among them. *BC* terms directly scale on conditional composites drawn in Fig. 7e–l, with signs imposed by changes in frequencies of Fig. 6b. For both models the increase in NAO+ and the decrease in AR frequencies both contribute to reduce the PP10 in AMIP-Future. The role of AR is significantly greater for IPSL, which results from the combination of a higher frequency decrease (Fig. 6b) and a greater conditional PP10 (Fig. 7h,l). Since models disagree on NAO− and BL evolutions, the corresponding *BC* terms are of opposite signs, especially for NAO− in Northern Europe. *WCd* terms are mostly negative for all models and regimes,

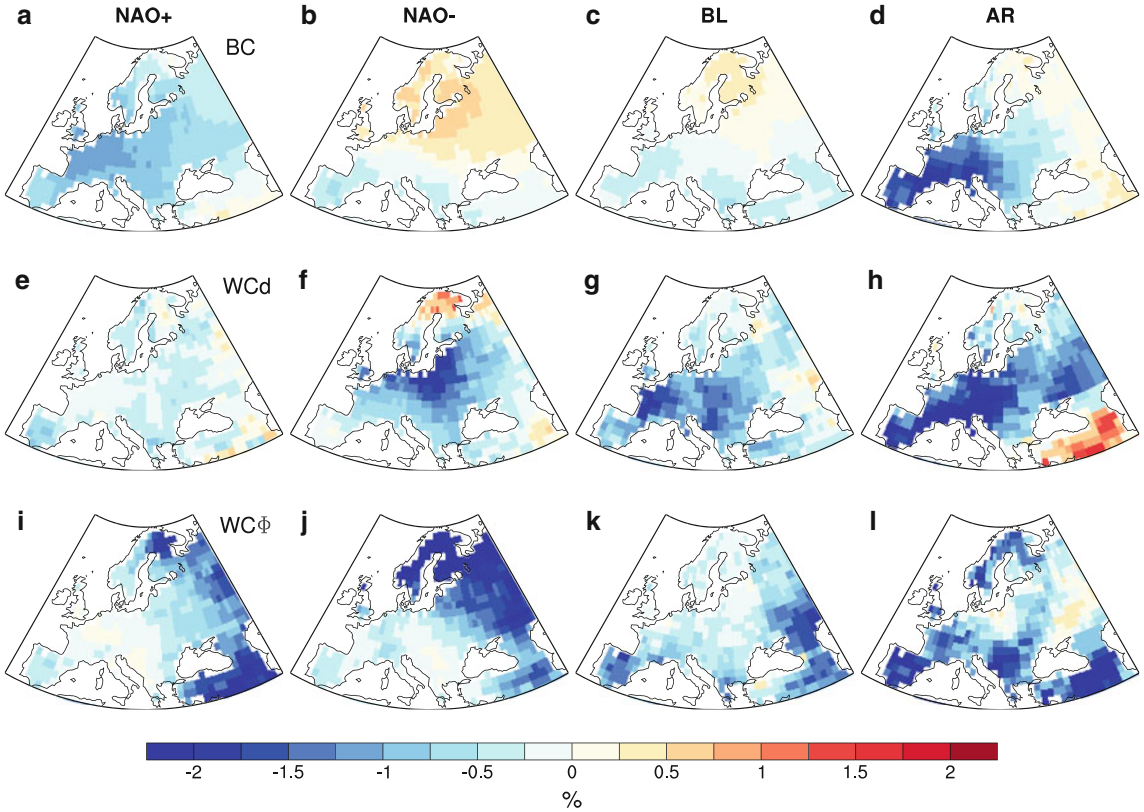


**Fig. 9** Same as Fig. 8 for IPSL. Units: %

indicating that the changes in Z500 distributions within weather regimes would reduce PP10 even with a constant transfer function Φ (e.g., unchanged regional physics). This also underlines that large-scale circulation changes would not have been totally accounted for if only considering them as changes in regime frequencies, as in (e.g., Goubanova et al. 2010), which highlights the interest of our linear model in Eq. 6. *WCd* contributions are more important for IPSL than for CNRM, which could be explained by the highest spatial heterogeneity in large-scale circulation changes (Fig. 4). Indeed, patterned changes found in IPSL hardly project onto regimes centroids, so that they are likely to induce larger changes in within-regime distributions, while CNRM changes in Z500 should more directly project onto NAO regimes frequencies. Eventually, *WC*Φ terms generally represent the highest contributions to PP10 decreases for all regimes, especially for CNRM. Logically, individual *WC*Φ contributions of each regime are the largest in areas where the regime is the most discriminating for PP10 (Fig. 7), and hence where changes in the Φ function are crucial for PP10. Interestingly, in some areas *WCd* changes are larger than *WC*Φ for the IPSL model, for example over Western Europe in BL and AR regimes. This could be interpreted as a prominent contribution of large-scale circulation changes to PP10 decrease in this model, but this probably reaches the limits of the artificial split introduced in Eq. 5 between Φ and *d*.

Absolute differences between Figs. 8 and 9 are plotted on Fig. 10. While terms in Fig. 10 do not sum as the total absolute difference between CNRM and IPSL (precisely because they are "absolute", not "raw" differences), they nevertheless highlight in which regime and/or which of *BC*, *WCd* and *WC*Φ terms the largest disagreements occur. In addition, such a measure could easily be extended to a greater ensemble of AMIP and/or CMIP simulations by replacing absolute values by standard deviations or variances, hence being helpful for investigating uncertainties in model responses to climate change. Here, largest uncertainties in the PP10 decrease occur in NAO− regime for Northern Europe and BL and AR regimes for Southern Europe, while both models agree reasonably well in NAO+ regime. In addition, uncertainties associated with changes in large-scale circulations, including NAO− and AR frequencies and BL and AR within-class distributions, have roughly the same influence on PP10 than uncertainties associated with changes in non-dynamical mechanisms (e.g., cloud and land surface feedbacks). While it should be interesting to test such conclusions with greater model-

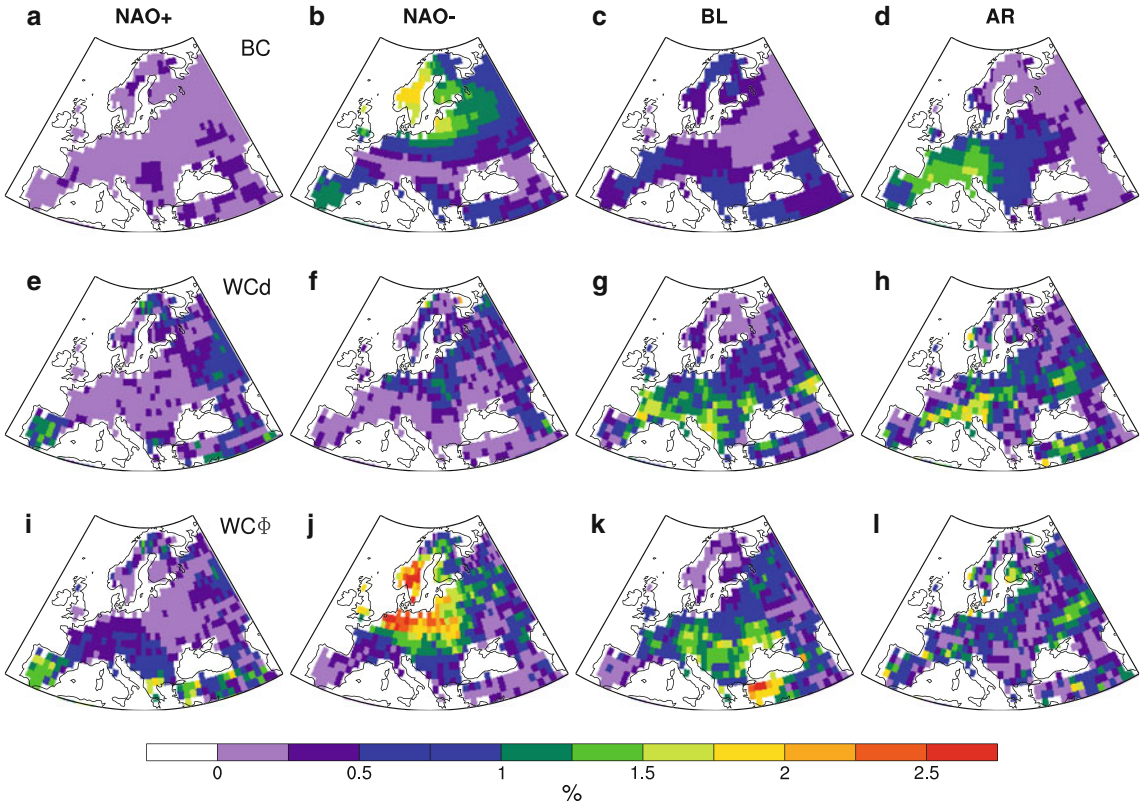


**Fig. 10** Absolute differences between Figs. 8 and 9. Units: %

ensembles, the large difference in simulated changes in regime frequencies between CNRM and IPSL possibly provides a rough preview of the model spread expected for large-scale changes.

## 4 Discussion and conclusions

In this paper we diagnose the representation of both mean and extreme wintertime European temperatures in idealized simulations of present-day and future climate performed with the CNRM and IPSL atmospheric GCMs. We find a cold (warm) mean bias for CNRM (IPSL), resulting in an overestimated (underestimated) probability of exceeding the observed 10th percentile (PP10). The sensitivity of both models to global warming exhibits similar features, albeit a slightly greater warming is found for CNRM, associated with a higher decrease in PP10. As wintertime European temperatures are mostly driven by the North-Atlantic chaotic dynamics, we use a weather-regime approach in order to evaluate the contribution of large-scale circulation to temperature errors and uncertainties. We find that observed frequencies of occurrence of all regimes are well captured by both models in the control AMIP experiments, with the exception of blocking episodes which are systematically underestimated. However, simulated frequencies differ in the AMIP-Future simulations: while both models suggest a more frequent NAO+ regime, they exhibit contrasted evolutions in NAO− and BL regimes, and IPSL shows a greater decrease in AR than CNRM does. Eventually, a linear breakdown methodology is proposed in order to split future changes in temperatures into contributions of large-scale circulation, including between- and within-regime changes, and non-dynamical mechanisms. This methodology applied on changes in PP10 reveals that most of the future decrease in PP10 is caused by changes in non-dynamical processes (including surface and radiative feedbacks), albeit large-scale circulation contributions can locally be of the same order of magnitude. The CNRM–IPSL difference in PP10 response, i.e. the model uncertainty, is dominated by uncertainties in both non-dynamical mechanisms and frequencies of NAO− and AR regimes.

The main issue when using weather regimes in order to investigate future changes in large-scale atmospheric circulation relies in discriminating structural changes, i.e. in spatial patterns, from a mere variation in the occurrence of the different regimes (Rust et al. 2010). Previous studies generally considered unchanged patterns in order to interpret changes in frequencies only (e.g., Goubanova et al. 2010). The flow-analog approach proposed here in order to also account for changes in within-regime circulation

distributions hence represents a step forward in the understanding of model uncertainties associated with large-scale dynamical processes. In addition, this breakdown methodology would probably gain to be applied to larger model ensembles and to both atmosphere-only (AMIP) and coupled ocean-atmosphere (CMIP) runs. To this aim, the dispersion found with AMIP-type runs and two models only indicates that greater model-ensembles could exhibit a large spread in the response of both large-scale circulations and temperatures to climate change. Also note that this methodology can be used for summer season as well, even if the ability of summer weather regimes to discriminate European temperatures is reduced.

Eventually, one of the main result in this paper is that the future warming in Europe, as well as the associated depletion in cold extremes, can not be explained by changes in regime frequencies only. Such a statement is in noted contradiction with studies published around the year 2000, after a period of anomalously frequent NAO+ conditions (Corti et al. 1999, among others; Palmer 1999, among others; Gillett et al. 2003, among others), but is consistent with more recent studies (Yiou et al. 2007; Vautard and Yiou 2009; Cattiaux et al. 2011). Note however that we have used idealized experiments in this study, in which changes in the surface energy budget simulated over Europe are strongly constrained by the prescribed 4 K global mean SST forcing. Applying our methodology to a global warming of smaller amplitude, e.g., 1979–2008 versus 2009–2028 or a faded scenario for the late twenty-first century, should reduce the contribution of non-dynamical mechanisms and emphasize the role of the North-Atlantic dynamics on long-term tendencies in European temperatures.

**Acknowledgments** The authors thank the two anonymous reviewers for helpful comments, and S. Tyteca (CNRM-GAME) who prepared the data used in this study. NCEP2 data are provided by the NOAA/OAR/ESRL PSD, USA (http://www.esrl.noaa.gov/psd/). EOBS data are provided by the EU-FP6 project ENSEMBLES (http://ensembles-eu.metoffice.com) and uses data of the ECA&D project (http://eca.knmi.nl). The research leading to these results has received funding by the European Union, Seventh Framework Program (FP7/2007–2013) under grant agreement #244067.

## References

Boé J, Terray L, Habets F, Martin E (2006) A simple statistical-dynamical downscaling scheme based on weather types and conditional resampling. J Geophys Res 111:D23106. doi:10.1029/2005JD006889

Cassou C (2008) Intraseasonal interaction between the Madden–Julian oscillation and the North Atlantic oscillation. Nature 455(7212):523–527. doi:10.1038/nature07286

Cassou C, Terray L, Phillips AS (2005) Tropical Atlantic influence on European heat waves. J Clim 18(15):2805–2811

Cattiaux J, Quesada B, Arakelian A, Codron F, Vautard R, Yiou P (2012) North-Atlantic dynamics and European temperature extremes in the IPSL model: sensitivity to atmospheric resolution. Clim Dyn (submitted)

Cattiaux J, Vautard R, Cassou C, Yiou P, Masson-Delmotte V, Codron F (2010a) Winter 2010 in Europe: a cold extreme in a warming climate. Geophys Res Lett 37:L20704. doi:10.1029/2010GL044613

Cattiaux J, Vautard R, Yiou P (2010b) North-Atlantic SST amplified recent wintertime European land temperature extremes and trends. Clim Dyn 36(11–12):2113–2128. doi:10.1007/s00382-010-0869-0

Cattiaux J, Yiou P, Vautard R (2011) Dynamics of future seasonal temperature trends and extremes in Europe: a multi-model analysis from CMIP3. Clim Dyn. Published online. doi:10.1007/s00382-011-1211-1

Corti S, Molteni F, Palmer TN (1999) Signature of recent climate change in frequencles of natural atmospheric circulation regimes. Nature 398(6730):799–802. doi:10.1038/19745

Déqué M, Marquet P, Jones RG (1998) Simulation of climate change over europe using a global variable resolution general circulation model. Clim Dyn 14(3):173–189. doi:10.1007/s003820050216

Deser C, Tomas R, Alexander M, Lawrence D (2010) The seasonal atmospheric response to projected arctic sea ice loss in the late twenty-first century. J Clim 23:333–351. doi:10.1175/2009JCLI3053.1

Douville H (2005) Limitations of time-slice experiments for predicting regional climate change over South Asia. Clim Dyn 24(4):373–391. doi:10.1007/s00382-004-0509-7

Driouech F, Déqué M, Sánchez-Gómez E (2010) Weather regimes—Moroccan precipitation link in a regional climate change simulation. Global Planet Change 72(1–2):1–10. doi:10.1016/j.gloplacha.2010.03.004

Dufresne JL et al (2012) Climate change projections using the IPSL-CM5 earth system model with an emphasis on changes between CMIP3 and CMIP5. Clim Dyn (submitted)

Franzke C, Woollings T, Martius O (2011) Persistent circulation regimes and preferred regime transitions in the North Atlantic. J Atmos Sci 68(12):2809–2825. doi:10.1175/JAS-D-11-046.1

Gillett NP, Zwiers FW, Weaver AJ, Stott PA (2003) Detection of human influence on sea-level pressure. Nature 422(6929):292–294. doi:10.1038/nature01487

Goubanova K, Li L, Yiou P, Codron F (2010) Relation between large-scale circulation and European winter temperature: does it hold under warmer climate? J Clim 3752–3760. doi:10.1175/2010JCLI3166.1

Haylock MR, Hofstra N, Klein Tank AMG, Klok EJ, Jones PD, New M (2008) A European daily high-resolution gridded data set of surface temperature and precipitation for 1950–2006. J Geophys Res 113:20119. doi:10.1029/2008JD10201

Hurrell JW, Kushnir Y, Ottersen G, Visbeck M (2003) The North Atlantic oscillation: climatic significance and environmental impact. American Geophysical Union, Washington, DC

Kanamitsu M, Ebisuzaki W, Woollen J, Yang SK, Hnilo JJ, Fiorino M, Potter GL (2002) NCEP-DOE AMIP-II reanalysis (R-2). Bull Am Meteorol Soc 83(11):1631–1643. ISSN 1520-0477

Kharin VV, Zwiers FW, Zhang X, Hegerl GC (2007) Changes in temperature and precipitation extremes in the IPCC ensemble of global coupled model simulations. J Clim 20(8):1419–1444

Kodra E, Steinhaeuser K, Ganguly AR (2011) Persisting cold extremes under 21st-century warming scenarios. Geophys Res Lett 38. doi:10.1029/2011GL047103

Lorenz EN (1969) Atmospheric predictability as revealed by naturally occurring analogues. J Atmos Sci 26(4):636–646

Menut L, Tripathi OP, Colette A, Vautard R, Flaounas E, Bessagnet B (2012) Evaluation of regional climate simulations for air quality modelling purposes. Clim Dyn. doi:10.1007/s00382-012-1345-9

Michelangeli PA, Vautard R, Legras B (1995) Weather regimes: recurrence and quasi stationarity. J Atmos Sci 52(8):1237–1256

Najac J, Boé J, Terray L (2009) A multi-model ensemble approach for assessment of climate change impact on surface winds in France. Clim Dyn 32:615–634. doi:10.&007/s00382-008-0440-4

Ouzeau G, Cattiaux J, Douville H, Ribes A, Saint-Martin D (2011) European cold winter of 2009/10: how unusual in the instrumental record and how reproducible in the Arpege-Climat model? Geophys Res Lett 38:L11706. doi:10.1029/2011GL047667

Palmer TN (1999) A nonlinear dynamical perspective on climate prediction. J Clim 12:575–591

Plaut G, Simonnet E (2001) Large-scale circulation classification, weather regimes, and local climate over France, the Alps and Western Europe. Clim Res 17(3):303–324

Rust HW, Vrac M, Lengaigne M, Sultan B (2010) Quantifying differences in circulation patterns based on probabilistic models. J Clim (in press). doi:10.1175/2010JCLI3432.1.

Sanchez-Gomez E, Terray L, Joly B (2008) Intra-seasonal atmospheric variability and extreme precipitation events in the European-Mediterranean region. Geophys Res Lett 35(15):L15708. doi:10.1029/2008GL034515

Scaife AA, Woollings T, Knight J, Martin G, Hinton T (2010) Atmospheric blocking and mean biases in climate models. J Clim 23:6143–6152

Stephenson DB, Pavan V, Collins M, Junge MM, Quadrelli R (2006) North Atlantic oscillation response to transient greenhouse gas forcing and the impact on European winter climate: a CMIP2 multi-model assessment. Clim Dyn 27(4):401–420. doi:10.1007/s00382-006-0140-x

Taylor KE, Stouffer RJ, Meehl GA (2007) A summary of the CMIP5 experiment design. World 4(December 2009):1–33

Thompson DWJ, Wallace JM (2001) Regional climate impacts of the Northern Hemisphere annular mode. Science 293(5527):85

van den Besselaar EJM, Klein Tank AMG, van der Schrier G (2010) Influence of circulation types on temperature extremes in Europe. Theoret Appl Climatol 99(3):431–439. doi:10.1007/s00704-009-0153-6

Vautard R (1990) Multiple weather regimes over the North Atlantic-analysis of precursors and successors. Mon Weather Rev 118(10):2056–81

Vautard R, Yiou P (2009) Control of recent European surface climate change by atmospheric flow. Geophys Res Lett 36(22):L22702. doi:10.1029/2009GL040480

Voldoire A, Sanchez-Gomez E, Salas y Melia D, Decharme B, Cassou C, Senesi S, Valcke S, Beau I, Alias A et al (2012) The CNRM-CM5.1 global climate model: description and basic evaluation. Clim Dyn. doi:10.1007/s00382-011-1259-y

Yiou P, Vautard R, Naveau P, Cassou C (2007) Inconsistency between atmospheric dynamics and temperatures during the exceptional 2006/2007 fall/winter and recent warming in Europe. Geophys Res Lett 34:L21808. doi:10.1029/2007GL031981